1

Kinetic and Thermodynamic Considerations for Photocatalyst Design

Frank E. Osterloh

University of California, Department of Chemistry, One Shields Avenue, Davis, CA 95616, USA

1.1 Introduction

Photochemical processes play a central role on Earth. While natural photosynthesis powers our biosphere and economic growth (through the use of photosynthesis-derived fossil fuels), additional photochemical processes are involved in shaping the "photogeochemistry" of our planet [1]. Light reactions play a role in the creation and function of the ozone ultraviolet (UV) filter in the atmosphere, the degradation of plant materials, man-made chemicals and plastics, and even in the chemical conversion of Earth-abundant minerals.

The potential of photochemical processes for technical applications was first demonstrated by A.E. Becquerel in 1839 when he discovered the photovoltaic effect. Interestingly, it took over a century before this knowledge was applied to practical photovoltaic cells [2]. In 1968, Gerischer's discovery of the dye sensitization effect at illuminated semiconductor surfaces [3] paved the way for Grätzel's construction of the first dye-sensitized photovoltaic cell 1991 [3] and also inspired for the production of hydrogen fuel from illuminated TiO₂ photoanodes [4, 5].

Since then, the interest in photochemical reactions for environmental remediation [6–10] and for the production of sustainable fuels has gained steadily [11–17]. In 2018, over 6000 articles were published with the term photocatalytic or photocatalyst in the title. This is about 60 times as many as published on this topic in 1991 when Grätzel's dye-sensitized solar cells made headlines. In contrast, the number of papers published on photosynthesis has been relatively steady in the past three decades, with approximately 1000 publications per year.

In the science community, photochemical reaction systems are typically referred to as "photocatalysts," or as "photosynthetic systems" or sometimes as devices for "artificial photosynthesis." Interestingly, there is no strong differentiation between these terms. For example, the International Union of Pure and Applied Chemistry (IUPAC) defines a "photocatalyst" as a "Catalyst able to produce, upon absorption of light, chemical transformations of the reaction partners. The excited state of

the photocatalyst repeatedly interacts with the reaction partners forming reaction intermediates and regenerates itself after each cycle of such interactions." [18] This definition makes no distinction between reactions that deposit photochemical energy in the products and reactions that do not.

According to Nozik [19] and Bard [20], excitonic reactions can be divided into photosynthetic and photocatalytic processes, depending on the thermodynamics of the associated reaction: [21].

"Photoelectrolytic cells ... can be classified as photosynthetic or photocatalytic. In the former case, radiant energy provides a Gibbs energy to drive a reaction such as $H_2O + H_2 + \frac{1}{2}O_2$, and electrical or thermal energy may be later recovered by allowing the reverse, spontaneous reaction to proceed. In a photocatalytic cell the photon absorption promotes a reaction with $\Delta G < 0$ so there is no net storage of chemical energy, but the radiant energy speeds up a slow reaction." [22]

As we will show here, this distinction between photocatalytic and photosynthetic devices becomes very significant to the understanding of their function and also to their optimization. An overview of the fundamental processes in photochemical reaction systems is presented in the following sections.

1.2 **Mechanistic Aspects of Photochemical Reaction Systems**

Photochemical (excitonic) reaction systems generally rely on the creation and transfer of charge carriers to induce the transformation of reagents in the vicinity of the light absorber. Usually, the process begins with the absorption of one or several photons (step 1), as shown in Figure 1.1a. This generates photoelectrons and holes, which subsequently react with reagents (step 2) to produce products. These products may interact with the photocatalyst repeatedly to undergo further transformations or they may react to form the starting materials again.

A very important aspect of a photochemical reaction system is the energy balance of the overall process. Two outcomes are possible, theoretically. In the first one, the products have a greater free energy than the reagents and the Gibbs free energy change for the process is positive, $\Delta G > 0$. An example for this kind of reaction is the photochemical water splitting reaction that produces hydrogen and oxygen. This process has a reaction free energy change of +237 kJ per mol of water, i.e. it is highly endergonic, as intended for a fuel forming reaction.

$$H_2O \rightarrow H_2 + O_2$$
, $\Delta G = +237$ kJ mol

In the second outcome, the products have a lower combined Gibbs free energy content than the reagents and the overall process is exergonic, $\Delta G < 0$. An example of the second type is the photochemical oxidation of organic matter into carbon dioxide and water, which is highly exergonic, because of the formation of CO2

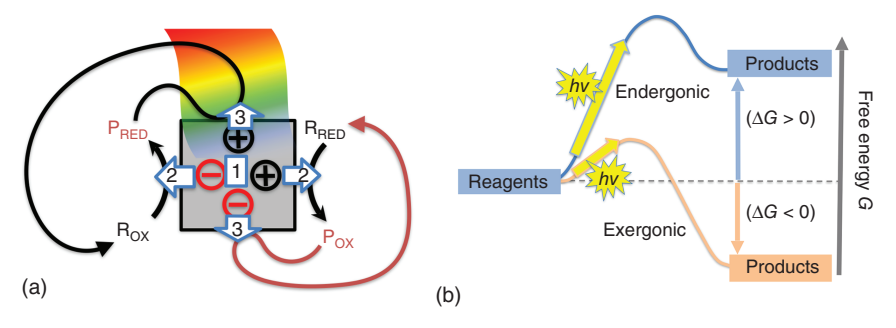


Figure 1.1 (a) General photochemical reaction system, including generation of photochemical charge carriers (1), electrochemical forward reactions (2), and backward (3) reactions. (b) Energetics of photochemical reactions. Source: Osterloh [23]. © 2017, American Chemical Society.

 $(\Delta G_F = -394.4 \text{ kJ mol}^{-1})$ and H_2O ($\Delta G_F = -228.6 \text{ kJ mol}^{-1}$). For example, the Gibbs free energy change for the combustion of propane is $-2.074 \text{ MJ mol}^{-1}$.

$$C_3H_8 + 5O_2 \rightarrow 4H_2O + 3CO_2$$
, $\Delta G = -2.074 \text{ MJ mol}^{-1}$

The difference in energetics for these processes has an important consequence on the design of the reaction system. If the forward process is endergonic, there is also a need to prevent the reverse thermodynamically favored reaction. This is shown in Figure 1.1b. Because the reaction products are at higher Gibbs free energy than the reagents, they may reform the starting materials, either by direct reaction or with the aid of the "photocatalyst." This limitation does not apply to exergonic processes, which cannot be reversed without additional energy input. Therefore, the ability to prevent the reverse, thermodynamically favored reaction is an important attribute of photochemical reaction systems that promote endergonic reactions.

Thus, in analogy to photoelectrochemical systems (see above), photochemical reaction systems can be classified as either **photosynthetic** when they promote endergonic (fuel forming) reactions or as **photocatalytic** when they promote exergonic, thermodynamically favored reactions. The efficiency of a fuel producing device is normally assessed with the energy efficiency of the process, i.e. the amount of photochemical energy stored in the reaction products [24]. For a photocatalytic device, on the other hand, the apparent quantum efficiency and the product selectivity are more suitable for assessing performance.

Because they have differing functions, it is expected that design of photosynthetic and photocatalytic devices will also be different. In this regard, it is useful to analyze a general photochemical process with specific emphasis of the ways for this reaction to become reversed. Let the photochemical reaction system in Figure 1.1a be that of the endergonic process I where an oxidized reagent $R_{\rm OX}$ and a reduced reagent $R_{\rm RED}$ are being converted into a reduced product $P_{\rm RED}$ and an oxidized product $P_{\rm OX}$. For natural photosynthesis, for example, $R_{\rm OX}=CO_2$ and $R_{\rm RED}=H_2O$ and $P_{\rm RED}=\{{\rm CHOH}\}$ (sugar fragment) and $P_{\rm OX}=O_2$.

At a minimum, this conversion must involve steps **II-IV**, where step **II** is the absorption of one or several photons to produce one or several electrons and holes

with a lifetime sufficient to react in steps III and IV. Step III uses the photoelectron to reduce R_{OX} to P_{RED} and step **IV** uses the photohole to oxidize R_{RED} to P_{OX} .

- (I) $R_{OX} + R_{RED} \rightarrow P_{RED} + P_{OX} \Delta G > 0$
- (II) Cat + $h\nu \rightarrow e^- + h^+$
- (III) $R_{OX} + e^- \rightarrow P_{RED}$
- (IV) $R_{RED} + h^+ \rightarrow P_{OX}$

After step IV, the photochemical reaction cycle can begin anew with the absorption of more photons.

Once products have been formed in sufficient quantity, the thermodynamically favored backreaction becomes increasingly favorable. It may proceed via reaction paths V-VII. If the products of the reaction are kinetically labile, they may react directly with each other to reform the original reagents, according to step V. This would be possible if the products are free radicals or radical intermediates, for example, superoxide (O2-) or partially reduced carbon compounds (e.g. methyl radical). Such radicals often form as intermediates in multistep photochemical conversion reactions, such as methanol synthesis from carbon dioxide.

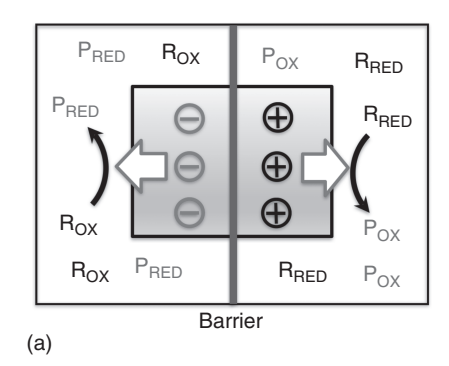
However, when the products are kinetically inert against direct reaction with each other (for example, H₂/O₂ from the water splitting reaction), the reverse reaction must occur via steps VI or VII. Here, the reduced product (e.g. H₂) might get oxidized by additional photoholes in the light absorber, or the oxidized product (e.g. O₂) might get reduced by additional photoelectrons.

- (V) $P_{RED} + P_{OX} \rightarrow R_{OX} + R_{RED} \Delta G < 0$ (direct backreaction)
- (VI) $P_{RED} + h^+ \rightarrow R_{OX}$ (oxidation of reduced product)
- (VII) $P_{OX} + e^- \rightarrow R_{RED}$ (reduction of oxidized product)

These backreactions can occur when the products of the photosynthetic reaction come into contact with hole and electron-donating sites at the light absorber, as shown in Figure 1.1a. These reactions must be prevented in order for the endergonic reaction to proceed in the forward direction. No such strict requirement exists for exergonic processes, for example, photocatalytic dye degradation, because there is no thermodynamic driving force for this process to reverse.

In principle, there are two different strategies to prevent reactions V-VII from occurring. In the first one (Figure 1.2), the backreaction is prevented by spatially separating the half reactions III and IV of the overall photochemical process from each other. This involves separating the products of the forward reaction and separating the charge carriers involved in them. Because the half reactions occur in different areas of the photochemical reaction system, any cross talk between them is prevented. This can be achieved by creating a physical barrier between reducing and oxidizing sites on the light absorber that prevents mixing of the products and reactions between them. The barrier action also extends to the photochemical charge carriers, which need to be separated so that they can reach the spatially distinct reaction sites of the light absorber.

The photoelectrochemical water splitting cell in Figure 1.2b is an example of this kind of reaction system. Anodic and cathodic reactions occur in separate



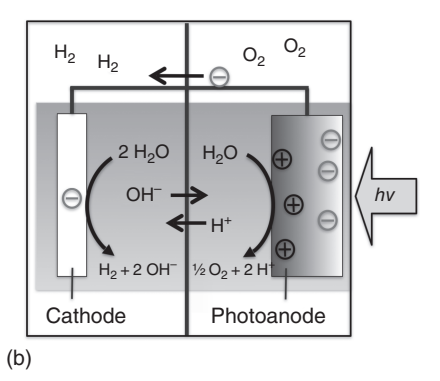


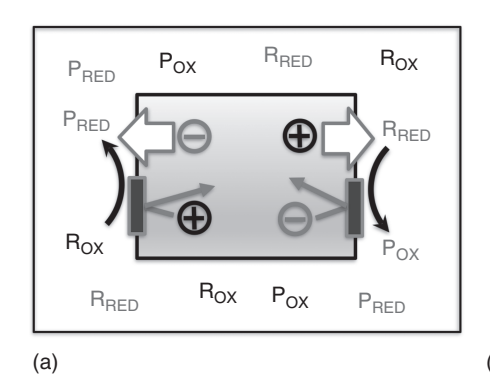
Figure 1.2 (a) Photochemical reaction system with separate compartments for anodic and cathodic processes. A barrier prevents mixture of reagents and products and of positive and negative charge carriers. (b) Photoelectrochemical water splitting cell as an example for this type of reaction system. Charge carriers are separated by the electric field at the solid-liquid junction of the photoanode. A membrane prevents mixing of H2 and O2 but allows transfer of hydroxide and/or protons and electrons and holes. Source: Osterloh [23]. © 2017, American Chemical Society.

compartments in the device, and electrons and holes are separated by the photoanode. No backreaction can occur because no electrons are available at the anodic side, and no holes at the cathode, and because H₂ and O₂ are physically separated in the two half cells. However, to allow the coupled electrochemical reactions to proceed, charge carriers and charge compensating ions must be able to transfer between the compartments.

A fundamentally different way to prevent the backreaction is shown in Figure 1.3a. Here, neither products nor charge carriers are separated, and all reactions occur inside of a single reaction compartment. Backreactions VI and VII are prevented by endowing the photochemical reaction sites with charge transfer selectivity. This charge transfer selectivity ensures that electrons can only be given to $\mathbf{R}_{\mathbf{O}\mathbf{X}}$ but not to P_{OX} and holes can only be transferred to R_{RED} but not to P_{RED} . Because the products are not separated, this type of reaction system can only be used if the products are sufficiently inert and will not react with each other according to reaction V.

The water splitting photocatalyst shown in Figure 1.3b is an example of a reaction system that exhibits electrochemical selectivity. Water oxidation and reduction take place on different sites on the photocatalyst, and product selectivity is achieved by preventing oxygen reduction with a Cr₂O₃ layer on top of the proton reduction site. No such precaution needs to be taken at the anodic reaction site, which is naturally selective for water oxidation because hydrogen oxidation is slow on most electrodes. Hydrogen and oxygen coevolution in the same sample space is possible because under the conditions of the water splitting reaction, the gas mixture is metastable with regard to the spontaneous formation of water. However, a spark can promote an explosion releasing the stored free energy. This means the gases will need to be separated in order to utilize them as fuels.

The design constraints specified in Figures 1.2 and 1.3 do not apply to exergonic photochemical reaction systems, such as a dye degradation photocatalyst. The



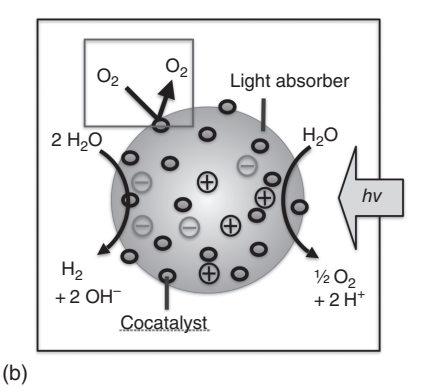


Figure 1.3 (a) Photochemical reaction system exhibiting charge transfer selectivity for anodic and cathodic processes that prevents oxidation of reduced product and reduction of oxidized products. (b) Example of a particle-based water splitting system for the production of H_2 and O_2 in a single compartment. Selective proton reduction is achieved by encasing the proton reduction site in a Cr_2O_3 shell that prevents photoreduction of oxygen. Source: Osterloh [23]. © 2017, American Chemical Society.

photocatalysts for such exergonic reactions are not susceptible to catalyzing the backreaction. Therefore, photocatalysts can operate on the basis of the general scheme in Figure 1.1a without the strict requirement for spatial separation of half reactions or charge transfer selectivity.

As Table 1.1 shows, most existing photochemical reaction systems can be classified as **exergonic**, or as **endergonic with charge selectivity** or **endergonic with spatial separation** of products and charge carriers. The list includes various types of photochemical water splitting systems [43, 44], which can be designed as spatially separated or as charge-selective devices. For example, the electrochemical cell with photovoltaic input would be a spatially separate photosynthetic device because carriers are separated in the solar cell and delivered to separate electrodes. On the other hand, a tandem (or *z*-scheme) of light-activated water oxidizing and water reducing particles in the same compartment would require electrochemical selectivity because both products (H_2 and O_2) are generated in the same reaction compartment.

The literature also contains many examples of suspended photocatalysts that produce $\rm H_2$ or $\rm O_2$ in the presence of a sacrificial donor or acceptor, which act as electron sources or sinks, respectively [45, 46]. Often, the addition of these reagents turns an endergonic process into an exergonic one, which means that no photochemical energy is deposited into the products. Examples are the photocatalytic water oxidation in the presence of $\rm Ce^{4+}$ as an extremely strong electron acceptor ($E^{\rm o}=+1.72\,\rm V$) or water reduction in the presence of sulfite ($E^{\rm o}=-0.93\,\rm V$ in basic solution) or methanol. However, when the sacrificial donor is a mild reducing agent, the overall process may still be endergonic. For example, $\rm H_2$ evolution (0.0 V RHE) from a $\rm SrTiO_3:Rh/Pt/[Fe(CN)_6]^{3-/4-}$ system (+0.36 V RHE) is endergonic because there is a net gain of 0.36 eV per transferred electron [47]. In photoelectrosynthetic cells, the sacrificial reagent is substituted by a voltage bias. This bias needs to be considered in calculating the photosynthetic efficiency of the system [44].

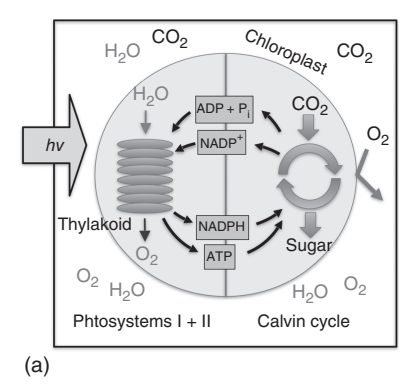
 Table 1.1
 Types of photochemical conversion devices [23].

		Endergonic, $\Delta G > 0$ (photosynthetic)	Endergonic, $\Delta G > 0$ (photosynthetic), electrochemically	Exergonic, $\Delta G < 0$
Process	Device	spatially separate	selective	(photocatalytic)
Water photoelectrolysis: $H, O \rightarrow H, + V_2O, : \Delta G > 0$	Electrochemical cell with photovoltaic power input [25, 26]	×		
1	Photoelectrochemical cell with photocathode or photoanode or both [27]	×		
	Suspension or film of single absorber particles [28]		X	
	Suspension or film of tandem absorber particles in one compartment [29, 30]		X	
	Tandem absorber particles in two compartments [31, 32]	X		
H_2 evolution from proton reduction with reducing agent (sacrificial donor):	Particle suspension/solution [33]			×
$H_2O + Red \rightarrow H_2 + Ox;$ $\Delta G < 0$				
O_2 evolution from water with chemical oxidizer (sacrificial acceptor): $H_2O + Ox \rightarrow O_2 + Red$;	Particle suspension/solution [34]			×
$\Delta G < 0$				
Natural photosynthesis: $6CO_2 + 6H_2O \rightarrow C_6H_{12}O_6 + O_2;\Delta G \!>\! 0$	Cyanobacteria, algae, plants [35]	×	×	

Table 1.1 (Continued)

Process	Device	Endergonic, $\Delta G > 0$ (photosynthetic) spatially separate	Endergonic, $\Delta G > 0$ (photosynthetic), electrochemically selectrive	Exergonic, $\Delta G < 0$ (photocatalytic)
CO ₂ reduction with reducing agent (sacrificial donor): CO, + Red + H, O \rightarrow CH, O, + Ox; $\Delta G < 0$	Particle suspension/solution [36, 37]			×
Oxidative degradation of dyes: $dye + O_2 \rightarrow Ox; \Delta G < 0$	Particle suspension/solution [38, 39]			×
Oxidation of NO _x : 2 NO + 3/2 O ₂ + H ₂ O \rightarrow 2 HNO ₃ ; $\Delta G < 0$	Particle suspension [40]			×
Nitrogen fixation with reducing agent Red + N_2 + $H_2O \rightarrow Ox + NH_3$; $\Delta G < 0$	Particle suspension/solution [41]			×
Oxidative C-H activation $R_3C-H+O_2 \rightarrow products+H_2O; \Delta G < 0$	Particle suspension/solution [42]			×
C–C and C–N coupling	Particle suspension/solution			X

Source: Adapted from https://pubs.acs.org/doi/abs/10.1021%2Facsenergylett.6b00665.



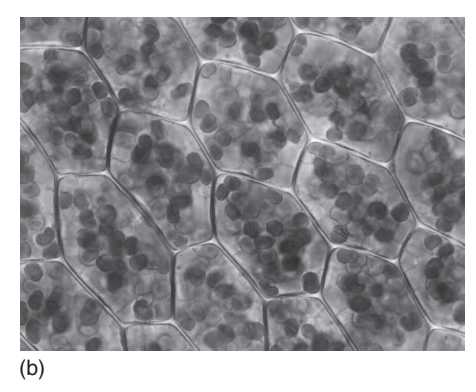


Figure 1.4 (a) Natural photosynthesis as a photochemical reaction system that employs separation of half reactions in addition to electrochemical selectivity. Source: Osterloh [23]. © 2017, American Chemical Society. (b) Plant cells with visible chloroplasts (from a moss, Plagiomnium affine). Source: Kristian Peters (https://en.wikipedia.org/wiki/Photosynthesis).

Difficult reactions with inert reagents (synthesis of ammonia from N₂ and protons) [42] or with complex reaction mechanism (CO₂ reduction to methane) [48–50] and in C-H activation or C-C or C-N coupling reactions often require a strong thermodynamic bias in the form of a powerful reducing agent or an applied voltage bias to achieve the desired outcome [51-53]. However, this applied bias may change the nature of the overall process from an energy-creating to an energy-consuming one, which cannot be tolerated if the goal is the production of fuels, such as methane or hydrogen.

Photochemical reactions that use oxygen as an abundant electron sink are also often thermodynamically favored. Examples of this type are the oxidative activation of methane or many processes for environmental remediation (degradation of organic compounds and nitrogen oxides, NO_x) [6, 9, 40, 54, 55] These reactions generate highly reactive hydroxyl and superoxide radicals that can abstract hydrogen atoms from hydrocarbons, causing various follow up reactions, and complete mineralization in some cases. Because of the oxidizing character of O_2 ($E^0 = +1.23 \text{ V}$ vs. reversible hydrogen electrode [RHE]), the thermodynamics are usually downhill and the backreaction is not a significant problem.

Clearly, natural photosynthesis in Table 1.1 belongs to the class of endergonic reactions. The process is carried out by plants and phytoplankton (algae and cyanobacteria). These photosynthetic cells utilize both chemical selectivity and spatial separation of the half reactions to achieve its function [35]. As can be seen schematically in Figure 1.4, plant cells have two separate compartments for the carbon-reducing half reaction (Calvin cycle) and the light-driven water oxidation reaction. The connection between the subsystems is achieved through the electron transport chain and various channels that move protons, ADP/ATP, and NADP/NADPH across the cell.

The problem of natural photosynthesis is that the permeability of the cell walls allows oxygen to enter into the Calvin cycle where it can be reduced preferentially over CO2. This oxygen reduction reaction is the first step of the backreaction of photosynthesis. Plants have learned to suppress it by a process called photorespiration [56, 57]. Here, enzymes are employed to remove oxygen reduction products from the Calvin cycle and to improve the selectivity toward glucose. Additionally, water oxidation at the oxygen evolving complex is very selective. This shows that natural photosynthesis employs charge transfer selectivity together with spatial separation of the half reactions.

1.3 Common Parameters of Photochemical Reaction **Systems**

The above classification of photochemical reaction systems allows a more detailed description of the parameters that limit each system type. All systems have in common that they rely on the absorption of photons, the generation of charge carriers, and the reaction of these carriers with reagents. These functions are enhanced by large absorption coefficients, long excited state/carrier lifetimes, and fast electrochemical reaction kinetics (low overpotentials), as summarized in Figure 1.5. The importance of these parameters is supported by experimental evidence.

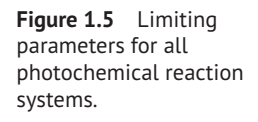
For example, it is well known that the photochemical water splitting rate of the GaN:ZnO particle catalyst is a function of the absorption coefficient of the material [58]. As shown in Figure 1.6a, photons with energies near the bandgap energy of the material are only weakly absorbed causing a low apparent quantum efficiency for water splitting. Higher photon energies can excite the material more effectively causing a higher apparent quantum efficiency. A similar dependence on the absorption coefficient has been demonstrated for molecular hydrogen evolution catalysts [59], for Rh-doped SrTiO₃ nanocrystals [47], for various photoelectrodes [60, 61], and for photovoltaic devices [62, 63]. Also, for natural photosynthesis (Figure 1.6b), the carbon fixation rate P is empirically linked to the absorption coefficient of chlorophyll α_{Chl} , the chlorophyll concentration C, the photosynthetic quantum efficiency Φ_m , and the irradiance E [56, 64].

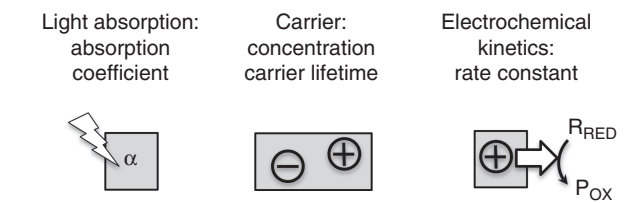
$$P^C = C \times \alpha_{\text{Chl}} \times \Phi_m \times E$$

This confirms the absorption coefficient as a limiting parameter across a set of inorganic, molecular, and biological photochemical reaction systems.

The second important parameter in Figure 1.5 is the lifetime τ (or decay time) of the photochemical charge carriers. This time is defined as the point when 1/e of the photochemical charge carriers has disappeared [63]. The value can be measured using microwave conductivity [65] or with transient absorption spectroscopy [66] by following the concentrations of excess electrons and holes after turning off the light. The longer τ , the greater the chance for the carriers to make their way to the reagents and the greater the photochemical reactivity.

The importance of the carrier lifetime is best established for photovoltaic devices, where it is well documented that short lifetimes caused by carrier recombination diminish the energy conversion efficiency of the device [62]. A similar correlation





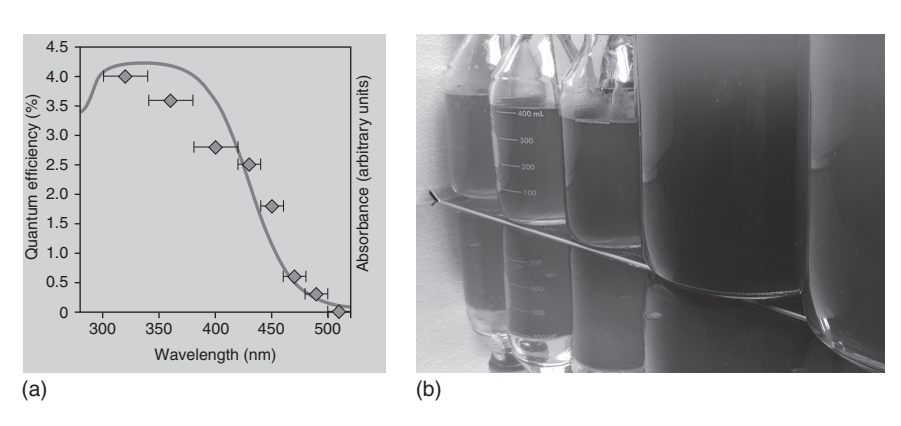


Figure 1.6 (a) Effect of optical absorbance on apparent quantum efficiency of photochemical water splitting with GaN:ZnO. Source: Maeda et al. [58]. © 2006, Springer Nature. (b) Variable light absorption in algae suspensions. Source: With permission from Kayla Rude and Professor Annaliese Franz, Department of Chemistry, University of California, Davis, USA.

has also been confirmed for photoelectrochemical cells [66–68], inorganic and [69–72] molecular photocatalysts [73–76], and natural photosynthesis [77, 78].

Lastly, as can be inferred from Figure 1.1, the photochemical activity depends on the kinetics of charge transfer. The rate constant for a simple electron transfer reaction is described by the Butler–Volmer equation [48, 79–84]. The constant k_f depends on the free energy of activation and on the thermodynamic driving force for the process, as defined by the reduction potential E of the electron donor and the standard reduction potential E^0 of the electron acceptor.

$$k_{f} = A_{f} \exp \left[\frac{-\Delta G_{o,c}^{\pm}}{RT} \right] \exp \left[\frac{-\alpha F \left(E - E^{0} \right)}{RT} \right]$$

This is illustrated in Figure 1.7 for charge transfer from an illuminated CdSe quantum dot to protons. The larger the bandgap and the more reducing the CdSe conduction band edge, the faster the proton reduction rate. This is an additional kinetic aspect of the general thermodynamic requirement that only those semiconductors whose conduction and valence band edges straddle the water reduction and oxidation potentials can promote the overall water splitting reaction [87].

Cocatalysts added to the light absorbers are known to speed up complex redox reactions such as the four-electron water oxidation [88] or the eight-electron CO₂ reduction to methane [50]. The cocatalyst changes the mechanism for the redox

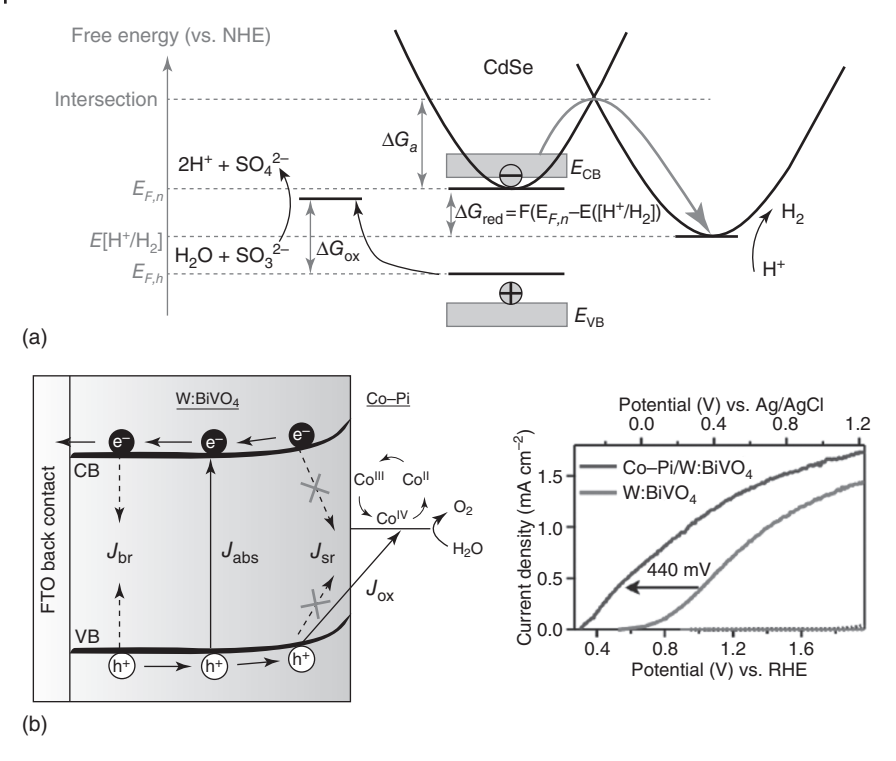


Figure 1.7 (a) Energetics of H_2 evolution from CdSe quantum dots with sulfite as a sacrificial electron donor. The conduction band edge becomes more reducing with decreasing nanocrystal size, promoting the proton reduction reaction. Source: Zhao et al. [85]. © 2013, American Chemical Society. (b) Effect of Co–Pi cocatalyst on photoelectrochemical water oxidation with BiVO₄. Source: Zhong et al. [86]. © 2011, American Chemical Society.

reaction, thereby altering the value of the activation free energy for charge transfer. This is illustrated in Figure 1.7b for water oxidation at an illuminated $BiVO_4$ surface with or without added Co–Pi catalyst (Co–Pi stands for cobalt phosphate). The presence of Co–Pi leads to higher photocurrents and a lower overpotential for water oxidation. Additionally, the plot demonstrates the effect of the electrochemical driving force on the photocurrent. As the applied anodic bias E becomes more positive, the rate constant for electron transfer increases exponentially, as seen in the Butler-Volmer equation.

Instead of a voltage bias, particle-based photochemical reaction systems often employ a chemical bias in the form of sacrificial reagents. Electron-donating reagents (hydrosulfide, methanol, and $\rm H_2O_2$) make the oxidation reaction thermodynamically and kinetically more favorable because they form stable reaction products (disulfide, CO, or $\rm O_2$, respectively) in fast reactions. This increases the photon conversion rate of suspended photocatalysts [46, 87, 89, 90] and the anodic photocurrent from $\rm Fe_2O_3$ [91], $\rm BiVO_4$ [92], and $\rm WO_3$ photoelectrodes [93]. The addition of fast electron acceptors such as $\rm AgNO_3$ [94], $\rm NaIO_4$ [95], or methylviologen dichloride similarly increases the cathodic photocurrent or

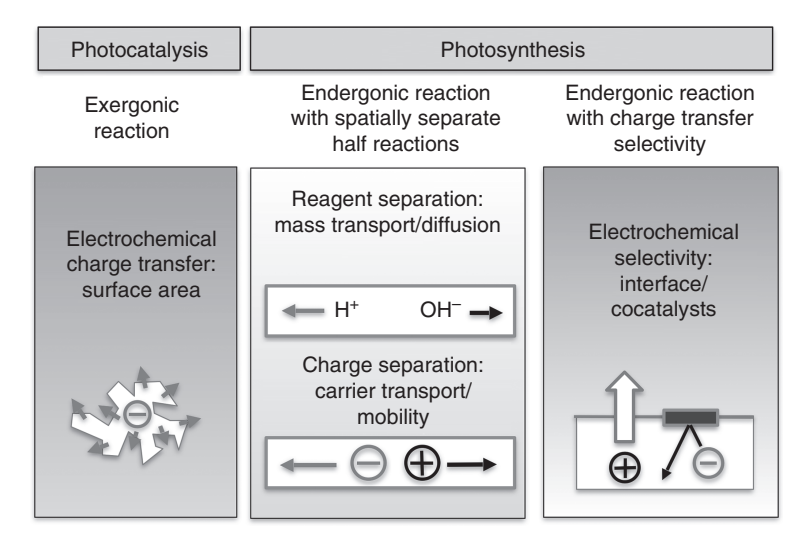


Figure 1.8 Sensitivity differences of photocatalytic and photosynthetic devices. Source: Adapted from Osterloh [23].

the oxygen evolution rate of suspended BiVO₄ [34], Fe₂O₃, [96] or NiO [97] photocatalysts.

1.4 Differences Between Photocatalytic and Photosynthetic Reaction Systems

Under conditions of optimal light absorption coefficients, long carrier lifetimes, and high electrochemical rate constants, photocatalysts and photosynthetic systems are limited by a set of complementary parameters. These are shown schematically in Figure 1.8.

Because they do not have to suppress the thermodynamically favored backreaction, photocatalysts are generally expected to perform better if their specific surface area is increased. This is a direct result of the fact that the heterogeneous charge transfer rate is an extensive property, which scales with the contact area between the charge donor and acceptor. This is well established for electrochemical reactions in general [79, 98].

Also, there are many examples in the literature that confirm the role of the specific surface area on reaction rate. For example, it is found that the photocatalytic hydrogen evolution rate of CdS [99], g- C_3N_4 [14, 100], KCa₂Nb₃O₁₀, and TiO₂ [101], in the presence of sacrificial electron donor increases with surface area. The same also applies to the photocatalytic dye degradation reaction with suspended metal oxide particles (Figure 1.9b) [102]. Under conditions of small specific surface area, the reactivity is limited by access of the reagents to the photocatalyst surface. This limitation is less applicable when the surface area is large, and other factors become limiting. However, it should be noted that dye decolorization experiments are also

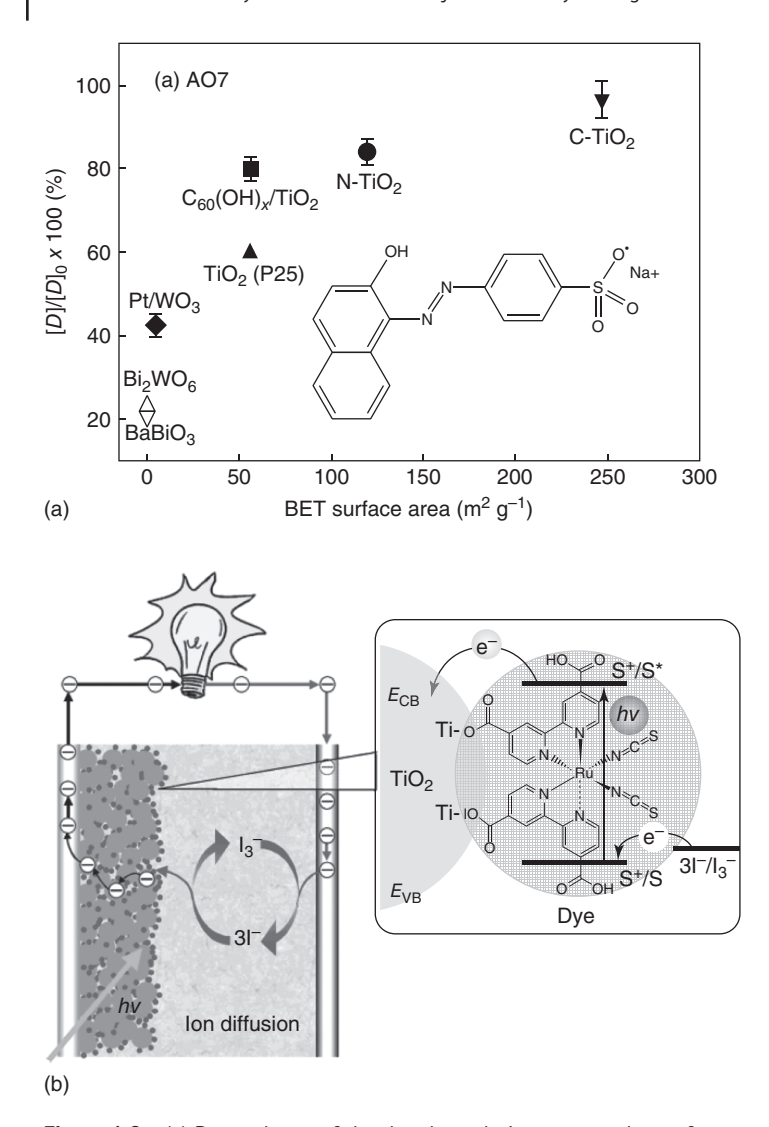


Figure 1.9 (a) Dependence of the dye degradation rate on the surface area of the photocatalyst. Source: Bae et al. [102]. © 2014, Elsevier. (b) Charge separation at the TiO_2 -dye-electrolyte interface. Source: Gratzel [103]. © 2005, American Chemical Society.

affected by the dye adsorption ability to the photocatalyst, competitive dye light absorption, and by the degradation mechanism, which varies from dye to dye, with solution pH, and with the photocatalyst [38, 102].

Similarly, it is found that the photocatalytic oxygen evolution rate for ${\rm Fe_2O_3}$ [96, 104] and ${\rm WO_3}$ [105, 106] increases with surface area. As a result, the highest activities are often found for nanostructured photoelectrodes of these materials. However, there are exceptions to the surface area – activity correlation. For example, quantum size effects in CdSe particles change the electronic structure of the material as

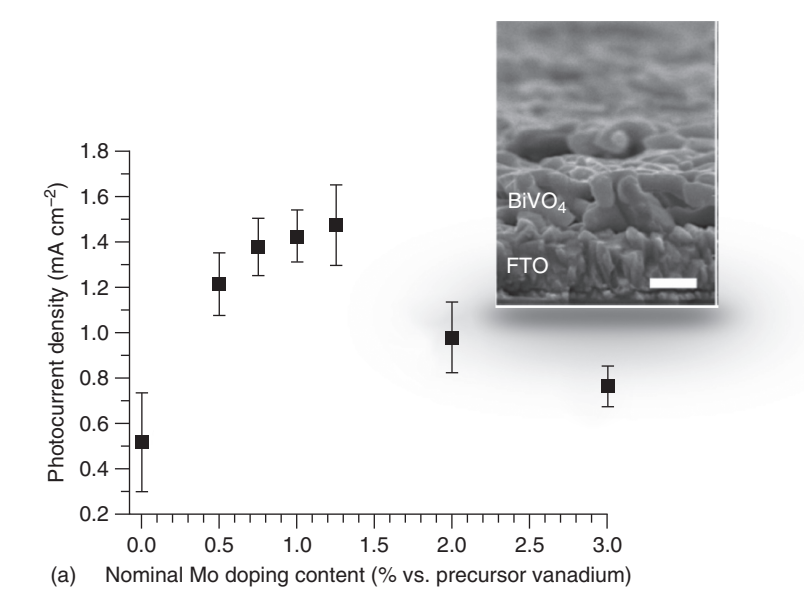
the crystal dimension is reduced [85]. This modifies the electron transfer rate constant and the light absorption coefficient, as discussed above. Often, it is also found that larger surface area causes a reduction in the electron-hole lifetimes, which will reduce the photocatalytic activity. This is usually a result of mid bandgap defects present at the surface of the photocatalyst [72].

Based on the surface area argument, the largest activity is expected for molecular photocatalysts that have the largest contact area with regard to the reagents. A good proof for this statement is iodide to tri-iodide oxidation in dye sensitized solar cells (Figure 1.9b). For such systems, the quantum efficiency is approaching 100%, i.e. nearly every photon results in oxidation of iodide and electron injection into the conductive support [107]. This remarkable behavior is due to the fact that the molecular dye is perfectly juxtaposed between the iodide/tri-iodide redox couple and the conductive support. The quantum efficiency of molecular systems drops significantly for more difficult reactions, such as water oxidation [108] or for hydrogen evolution [76, 109]. This is because for these multielectron charge transfer reactions, the electrochemical kinetics of the conversion reaction become limiting [110, 111].

Next, we turn the discussion to photosynthetic devices that promote endergonic reactions such as the water splitting reaction (Figure 1.8). In contrast to photocatalytic reaction systems, these devices must also be able to suppress the reverse of the photosynthetic reaction. Photosynthetic devices that rely on spatial separation of the half reactions accomplish this task usually with a solid-solid (buried) or solid-liquid junction [112, 113]. For suspended systems, dipoles in the lattice [114, 115] or at the surface of the absorber also play a role in charge separation [116, 117]. Charge separation can become the limiting factor of a photosynthetic device because it depends on both the effectiveness of the junction and also on the mobility of the charge carriers that are moving across it [62, 63, 118].

This limitation is the reason for the often lower photoelectrochemical performance of early transition metal oxides (such as Fe₂O₃) [119] when compared to main group element semiconductors (such as silicon) [120, 121]. The latter have a much larger mobility of their charge carriers. For transition metal oxides, doping with electron donors is often employed to improve the mobility of the charge carriers. This is shown in Figure 1.10a for a BiVO4 water oxidation photoanode [61]. Addition of molybdenum or tungsten ions makes the material more n-type and allows extraction of majority carriers at the back contact [123]. For high Mo concentrations, defect recombination effects from the introduction of the Mo states begin to dominate. A similar behavior is seen for Si- and Ti-doped Fe₂O₃ photoanodes [124, 125].

Because charge separation is added as a functional requirement, the simple correlation of activity and the specific surface area is no longer valid in photosynthetic devices, and the nanostructuring approach is no longer effective [17]. For example, in SrTiO₃/Ni particles for the endergonic overall water splitting reaction, it is observed that product rates do not increase with smaller particle sizes and larger surface area. Instead, as the particles get smaller, separation of electrons and holes becomes more difficult [126]. Similarly, silicon nanowire arrays designed for



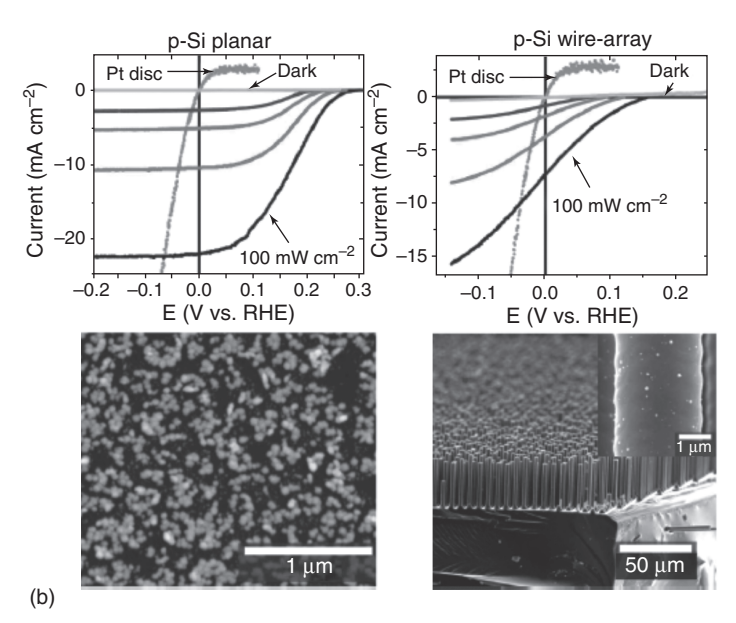


Figure 1.10 (a) Effect of Mo concentration on the photocurrent in $BiVO_4$ photoanodes for water oxidation. Source: Adapted from Seabold et al. [61]. © 2014, Royal Society of Chemistry. (b) Dependence of the proton reduction photocurrent and onset voltage on the surface morphology of the Si photoelectrode. Source: Reproduced from Boettcher et al. [122]. © 2011, American Chemical Society.

hydrogen evolution from water were found to produce lower photocurrents and to require higher bias voltages than their planar silicon analogs (Figure 1.10b) [122]. The lower performance of the high surface area nanorods is likely due to decreased electron hole separation resulting from the greater junction area [62].

A reduction in performance can also result when ion/mass transport connected to the Faradaic reaction is slow. This applies to two-compartment water splitting cells, where protons from the oxygen evolving half reaction need to reach the cathode for hydrogen evolution. Experimentally, it is found here that electrolyte cycling decreases diffusion potentials and increases the performance of the cell [32, 127]. The same consideration applies to natural photosynthesis. Under light-saturated conditions, the carbon fixation rate can be limited by either electron or mass transport in the Calvin cycle [57]. Additionally, transport of CO₂ to the reaction center can become rate limiting, which limits plant growth in dense forests without air circulation [56, 128].

These transport limitations are relaxed for photosynthetic devices that operate with electrochemical selectivity instead of spatial separation of the half reactions. Reducing charge transport pathways is particularly effective for transition metal oxides because of their lower carrier mobility and because their depletion regions are often on the nanoscale [119]. Also, in suspension systems, an effective charge separation mechanism is often missing because of the symmetry of the suspended particles and the difficulty of adding junctions and cocatalysts in a spatially controlled fashion [31]. Therefore, for suspended particle systems, electrochemical selectivity for fuel-generating reactions is often achieved with cocatalysts that are added to the surface of the light absorber. For example, Maeda et al. showed in 2006 that the water splitting performance of GaN:ZnO particles could be increased by integrating the absorber with a Rh/Cr₂O₃ cocatalyst for hydrogen evolution [129]. This cocatalyst was able to reduce protons but prevent the reduction of oxygen, which is the first step in the backreaction to water. The selectivity relies on the ability of the Cr₂O₃ layer to prevent access of molecular O₂ to the buried proton reduction site. Later evolutions of the catalyst use a $Rh_{2-\nu}Cr_{\nu}O_{x}$ composite that can be deposited onto the light absorber using an impregnation route [29, 130-134]. Similarly, in 2007, Kudo and coworkers demonstrated improved hydrogen evolution selectivity of Pt cocatalysts in the presence of $[Fe(SO_4)(H_2O)_5]^+$ and $[Fe(OH)(H_2O)_5]^{2+}$ complexes [135] or in the presence of carbonates [136] and iodide [137]. These reagents are believed to alter the Pt surface toward decreased oxygen reduction. The selective charge transfer strategy works for the water splitting reaction because in the absence of a suitable catalyst, hydrogen and oxygen are metastable with regard to water formation. However, additional energy is required to separate products, which can reduce the overall activity of the system [31].

1.5 Conclusion

The above analysis reveals that photochemical reaction systems can be classified into three categories, according to their function and operational principles:

- 1. Photocatalytic devices that promote exergonic processes
- 2. Photosynthetic devices that promote endergonic (fuel forming) processes by separating the half reactions
- 3. Photosynthetic devices that promote endergonic (fuel forming) processes by using charge transfer selectivity

All of these systems rely on the generation and transfer of photochemical charge carriers. Therefore, the activity of all of them increases with the light absorption coefficient, the excited state lifetime, and the electrochemical reaction kinetics. Because photocatalytic devices do not need to suppress the backreaction, their activity scales with the specific surface area. This means that better photocatalysts can be created by increasing the surface area or by decreasing the size of the light absorber. This does not apply to photosynthetic systems with spatially separate half reactions, which under conditions of optimized light absorption, carrier lifetimes, and charge transfer are limited by charge separation and charge and mass transport. Such devices can be improved by increasing the effectiveness of the junctions across the device and by raising the charge carrier mobility and mass transfer rates of reagents and reaction intermediates. On the other hand, the activity of photosynthetic systems that rely on charge transfer selectivity may be limited by this very selectivity. Such devices can be improved through modification of the interfaces and through engineering of more selective charge transfer cocatalysts.

Acknowledgment

Funding Sources

This material is based on the work supported by the National Science Foundation for financial support (CHE 1900136) and by the U.S. Department of Energy, Office of Science, Office of Basic Energy Sciences under Award Number DE-SC0015329.

The opinions are those of the author and do not necessarily reflect the views of the funding agencies.

References

- 1 Doane, T.A. (2017). A survey of photogeochemistry. Geochem. Trans. 18: 1.
- 2 Chapin, D.M., Fuller, C.S., and Pearson, G.L. (1954). A new silicon p-n junction photocell for converting solar radiation into electrical power. J. Appl. Phys. 25: 676-677.
- 3 Gerischer, H., Michel-Beyerle, M.E., Rebentrost, F., and Tributsch, H. (1968). Sensitization of charge injection into semiconductors with large band gap. Electrochim. Acta 13: 1509-1515.
- 4 Boddy, P.J. (1968). Oxygen evolution on semiconducting TiO2. J. Electrochem. Soc. 115: 199.

- 5 Fujishima, A. and Honda, K. (1971). Studies on photosensitive electrode reactions. 3. Electrochemical evidence for mechanism of primary stage of photosynthesis. Bull. Chem. Soc. Jpn. 44: 1148-1150.
- 6 Hoffmann, M.R., Martin, S.T., Choi, W.Y., and Bahnemann, D.W. (1995). Environmental applications of semiconductor photocatalysis. Chem. Rev. 95: 69-96.
- 7 Linsebigler, A.L., Lu, G.Q., and Yates, J.T. (1995). Photocatalysis on TiO₂ surfaces - principles, mechanisms, and selected results. Chem. Rev. 95: 735-758.
- 8 Fox, M.A. and Dulay, M.T. (1993). Heterogeneous photocatalysis. Chem. Rev. 93: 341-357.
- 9 Fujishima, A., Zhang, X.T., and Tryk, D.A. (2008). TiO₂ photocatalysis and related surface phenomena. Surf. Sci. Rep. 63: 515-582.
- 10 Kamat, P.V. (2002). Photophysical, photochemical and photocatalytic aspects of metal nanoparticles. J. Phys. Chem. B 106: 7729-7744.
- 11 Bard, A.J. and Fox, M.A. (1995). Artificial photosynthesis solar splitting of water to hydrogen and oxygen. Acc. Chem. Res. 28: 141-145.
- 12 Gratzel, M. (1981). Artificial photosynthesis water cleavage into hydrogen and oxygen by visible-light. Acc. Chem. Res. 14: 376-384.
- 13 Alstrum-Acevedo, J.H., Brennaman, M.K., and Meyer, T.J. (2005). Chemical approaches to artificial photosynthesis. 2. Inorg. Chem. 44: 6802-6827.
- 14 Wang, X.C., Maeda, K., Chen, X.F. et al. (2009). Polymer semiconductors for artificial photosynthesis: hydrogen evolution by mesoporous graphitic carbon nitride with visible light. J. Am. Chem. Soc. 131: 1680-1681.
- 15 Wasielewski, M.R. (1992). Photoinduced electron-transfer in supramolecular systems for artificial photosynthesis. Chem. Rev. 92: 435-461.
- 16 Gust, D., Moore, T.A., and Moore, A.L. (2009). Solar fuels via artificial photosynthesis. Acc. Chem. Res. 42: 1890-1898.
- 17 Osterloh, F.E. (2015). Nanoscale effects in water splitting photocatalysis. *Top.* Curr. Chem. 371: 105-142.
- 18 McNaught, A.D., Wilkinson, A., and International Union of Pure and Applied Chemistry (1997). Compendium of Chemical Terminology: IUPAC Recommendations, 2e, vii. Oxford Oxfordshire; Malden, MA: Blackwell Science, 450 p.
- **19** Nozik, A.J. (1977). Photochemical diodes. *Appl. Phys. Lett.* 30: 567–569.
- 20 Bard, A.J. (1979). Photoelectrochemistry and heterogeneous photocatalysis at semiconductors. J. Photochem. 10: 59-75.
- 21 Rajeshwar, K., Thomas, A., and Janaky, C. (2015). Photocatalytic activity of inorganic semiconductor surfaces: myths, hype, and reality. J. Phys. Chem. Lett. 6: 139-147.
- 22 Bard, A.J., Memming, R., and Miller, B. (1991). Terminology in semiconductor electrochemistry and photoelectrochemical energy-conversion - (recommendations 1991). Pure Appl. Chem. 63: 569-596.
- 23 Osterloh, F.E. (2017). Photocatalysis versus photosynthesis: a sensitivity analysis of devices for solar energy conversion and chemical transformations. ACS Energy Lett.: 445-453.

- 24 Chen, Z.B., Jaramillo, T.F., Deutsch, T.G. et al. (2010). Accelerating materials development for photoelectrochemical hydrogen production: standards for methods, definitions, and reporting protocols. J. Mater. Res. 25: 3-16.
- 25 Licht, S., Wang, B., Mukerji, S. et al. (2001). Over 18% solar energy conversion to generation of hydrogen fuel; theory and experiment for efficient solar water splitting (Reprinted from J. Phys. Chem. B, vol 104, pg 8920-8924, 2000). Int. J. Hydrogen Energy 26: 653-659.
- 26 Gratzel, M. (2001). Photoelectrochemical cells. Nature 414: 338-344.
- 27 Sivula, K. and van de Krol, R. (2016). Semiconducting materials for photoelectrochemical energy conversion. Nat. Rev. Mater. 1: 15010.
- 28 Maeda, K., Takata, T., Hara, M. et al. (2005). GaN:ZnO solid solution as a photocatalyst for visible-light-driven overall water splitting. J. Am. Chem. Soc. 127: 8286-8287.
- 29 Wang, Q., Hisatomi, T., Jia, Q. et al. (2016). Scalable water splitting on particulate photocatalyst sheets with a solar-to-hydrogen energy conversion efficiency exceeding 1%. Nat. Mater. 15: 611-615.
- 30 Kibria, M.G., Nguyen, H.P.T., Cui, K. et al. (2013). One-step overall water splitting under visible light using multiband InGaN/GaN nanowire heterostructures. ACS Nano 7: 7886-7893.
- 31 Fabian, D.M., Hu, S., Singh, N. et al. (2015). Particle suspension reactors and materials for solar-driven water splitting. Energy Environ. Sci. 8: 2825-2850.
- **32** Sasaki, Y., Kato, H., and Kudo, A. (2013). $[Co(bpy)_3]^{3+/2+}$ and $[Co(phen)_3]^{3+/2+}$ electron mediators for overall water splitting under sunlight irradiation using Z-scheme photocatalyst system. J. Am. Chem. Soc. 135: 5441-5449.
- 33 Buhler, N., Meier, K., and Reber, J.F. (1984). Photochemical hydrogen-production with cadmium-sulfide suspensions. J. Phys. Chem. 88: 3261-3268.
- 34 Wang, J. and Osterloh, F.E. (2014). Limiting factors for photochemical charge separation in BiVO₄/Co₃O₄, a highly active photocatalyst for water oxidation in sunlight. J. Mater. Chem. A 2: 9405-9411.
- **35** Barber, J. and Tran, P.D. (2013). From natural to artificial photosynthesis. J. R. Soc. Interface 10, http://dx.doi.org/10.1098/rsif.2012.0984.
- 36 Roy, S.C., Varghese, O.K., Paulose, M., and Grimes, C.A. (2010). Toward solar fuels: photocatalytic conversion of carbon dioxide to hydrocarbons. ACS Nano 4: 1259-1278.
- 37 Iwase, A., Yoshino, S., Takayama, T. et al. (2016). Water splitting and CO₂ reduction under visible light irradiation using Z-scheme systems consisting of metal sulfides, CoOx-loaded BiVO4, and a reduced graphene oxide electron mediator. J. Am. Chem. Soc. 138: 10260-10264.
- 38 Yan, X., Ohno, T., Nishijima, K. et al. (2006). Is methylene blue an appropriate substrate for a photocatalytic activity test? A study with visible-light responsive titania. Chem. Phys. Lett. 429: 606-610.
- 39 Kamimura, S., Miyazaki, T., Zhang, M. et al. (2016). (Au@Ag)@Au double shell nanoparticles loaded on rutile TiO2 for photocatalytic decomposition of 2-propanol under visible light irradiation. Appl. Catal. B Environ. 180: 255-262.

- 40 Ibusuki, T. and Takeuchi, K. (1994). Removal of low concentration nitrogen oxides through photoassisted heterogeneous catalysis. J. Mol. Catal. 88: 93-102.
- 41 Brown, K.A., Harris, D.F., Wilker, M.B. et al. (2016). Light-driven dinitrogen reduction catalyzed by a CdS:nitrogenase MoFe protein biohybrid. Science 352: 448-450.
- **42** Kisch, H. (2013). Semiconductor photocatalysis—mechanistic and synthetic aspects. Angew. Chem. Int. Ed. 52: 812-847.
- 43 Ager, J.W., Shaner, M.R., Walczak, K.A. et al. (2015). Experimental demonstrations of spontaneous, solar-driven photoelectrochemical water splitting. Energy Environ. Sci. 8: 2811-2824.
- 44 Coridan, R.H., Nielander, A.C., Francis, S.A. et al. (2015). Methods for comparing the performance of energy-conversion systems for use in solar fuels and solar electricity generation. Energy Environ. Sci. 8: 2886-2901.
- 45 Zhou, P., Yu, J.G., and Jaroniec, M. (2014). All-solid-state Z-scheme photocatalytic systems. Adv. Mater. 26: 4920-4935.
- 46 Schneider, J. and Bahnemann, D.W. (2013). Undesired role of sacrificial reagents in photocatalysis. J. Phys. Chem. Lett. 4: 3479-3483.
- 47 Wang, J., Zhao, J., and Osterloh, F.E. (2015). Photochemical charge transfer observed in nanoscale hydrogen evolving photocatalysts using surface photovoltage spectroscopy. Energy Environ. Sci. 8: 2970-2976.
- 48 Kortlever, R., Shen, J., Schouten, K.J.P. et al. (2015). Catalysts and reaction pathways for the electrochemical reduction of carbon dioxide. J. Phys. Chem. Lett. 6: 4073-4082.
- 49 Morris, A.J., Meyer, G.J., and Fujita, E. (2009). Molecular approaches to the photocatalytic reduction of carbon dioxide for solar fuels. Acc. Chem. Res. 42: 1983-1994.
- 50 Habisreutinger, S.N., Schmidt-Mende, L., and Stolarczyk, J.K. (2013). Photocatalytic reduction of CO2 on TiO2 and other semiconductors. Angew. Chem. Int. Ed. 52: 7372-7408.
- 51 Barton, E.E., Rampulla, D.M., and Bocarsly, A.B. (2008). Selective solar-driven reduction of CO2 to methanol using a catalyzed p-GaP based photoelectrochemical cell. J. Am. Chem. Soc. 130: 6342-6344.
- 52 Kumar, B., Llorente, M., Froehlich, J. et al. (2012). Photochemical and photoelectrochemical reduction of CO₂. In: Annual Review of Physical Chemistry, vol. 63 (eds. M.A. Johnson and T.J. Martinez), 541-569. Annual Reviews, doi: https://doi.org/10.1146/annurev-physchem-032511-143759.
- 53 Arai, T., Sato, S., and Morikawa, T. (2015). A monolithic device for CO₂ photoreduction to generate liquid organic substances in a single-compartment reactor. Energy Environ. Sci. 8: 1998-2002.
- 54 Shinde, S.S., Bhosale, C.H., and Rajpure, K.Y. (2013). Kinetic analysis of heterogeneous photocatalysis: role of hydroxyl radicals. Catal. Rev. 55: 79–133.
- 55 Marschall, R. (2014). Semiconductor composites: strategies for enhancing charge carrier separation to improve photocatalytic activity. Adv. Funct. Mater. 24: 2421-2440.

- 56 Blankenship, R.E., Tiede, D.M., Barber, J. et al. (2011). Comparing photosynthetic and photovoltaic efficiencies and recognizing the potential for improvement. Science 332: 805-809.
- 57 Zhu, X.-G., Long, S.P., and Ort, D.R. (2010). Improving photosynthetic efficiency for greater yield. Annu. Rev. Plant Biol. 61: 235-261.
- 58 Maeda, K., Teramura, K., Lu, D.L. et al. (2006). Photocatalyst releasing hydrogen from water - enhancing catalytic performance holds promise for hydrogen production by water splitting in sunlight. Nature 440: 295-295.
- **59** Wang, X., Goeb, S., Ji, Z. et al. (2011). Homogeneous photocatalytic hydrogen production using π -conjugated platinum(II) arylacetylide sensitizers. *Inorg.* Chem. 50: 705-707.
- 60 Maeda, K., Higashi, M., Siritanaratkul, B. et al. (2011). SrNbO₂N as a water-splitting photoanode with a wide visible-light absorption band. J. Am. Chem. Soc. 133: 12334-12337.
- 61 Seabold, J.A., Zhu, K., and Neale, N.R. (2014). Efficient solar photoelectrolysis by nanoporous Mo:BiVO4 through controlled electron transport. Phys. Chem. Chem. Phys. 16: 1121-1131.
- 62 Würfel, P. (2005). Physics of Solar Cells, 244. Weinheim: Wiley-VCH.
- 63 Dittrich, T. (2015). Materials Concepts for Solar Cells, xxxiii. London: Imperial College Press, 516 p.
- 64 MacIntyre, H.L., Kana, T.M., Anning, T., and Geider, R.J. (2002). Photoacclimation of photosynthesis irradiance response curves and photosynthetic pigments in microalgae and cyanobacteria. J. Phycol. 38: 17-38.
- 65 Abdi, F.F., Savenije, T.J., May, M.M. et al. (2013). The origin of slow carrier transport in BiVO₄ thin film photoanodes: a time-resolved microwave conductivity study. J. Phys. Chem. Lett. 4: 2752-2757.
- 66 Pendlebury, S.R., Cowan, A.J., Barroso, M. et al. (2012). Correlating long-lived photogenerated hole populations with photocurrent densities in hematite water oxidation photoanodes. Energy Environ. Sci. 5: 6304-6312.
- 67 Barroso, M., Cowan, A.J., Pendlebury, S.R. et al. (2011). The role of cobalt phosphate in enhancing the photocatalytic activity of alpha-Fe₂O₃ toward water oxidation. J. Am. Chem. Soc. 133: 14868-14871.
- 68 Pesci, F.M., Cowan, A.J., Alexander, B.D. et al. (2011). Charge carrier dynamics on mesoporous WO₃ during water splitting. J. Phys. Chem. Lett. 2: 1900-1903.
- 69 Hisatomi, T., Kubota, J., and Domen, K. (2014). Recent advances in semiconductors for photocatalytic and photoelectrochemical water splitting. Chem. Soc. Rev. 43: 7520-7535.
- 70 Zhang, F., Yamakata, A., Maeda, K. et al. (2012). Cobalt-modified porous single-crystalline LaTiO2N for highly efficient water oxidation under visible light. J. Am. Chem. Soc. 134: 8348-8351.
- 71 Ben-Shahar, Y., Scotognella, F., Waiskopf, N. et al. (2015). Effect of surface coating on the photocatalytic function of hybrid CdS-Au nanorods. Small 11: 462-471.

- 72 Amano, F., Ishinaga, E., and Yamakata, A. (2013). Effect of particle size on the photocatalytic activity of WO₃ particles for water oxidation. J. Phys. Chem. C 117: 22584-22590.
- 73 Zhao, J., Wu, W., Sun, J., and Guo, S. (2013). Triplet photosensitizers: from molecular design to applications. Chem. Soc. Rev. 42: 5323-5351.
- 74 Ohkubo, K. and Fukuzumi, S. (2009). Rational design and functions of electron donor-acceptor dyads with much longer charge-separated lifetimes than natural photosynthetic reaction centers. Bull. Chem. Soc. Jpn. 82: 303-315.
- 75 Imahori, H., Guldi, D.M., Tamaki, K. et al. (2001). Charge separation in a novel artificial photosynthetic reaction center lives 380 ms. J. Am. Chem. Soc. 123: 6617-6628.
- 76 Gärtner, F., Denurra, S., Losse, S. et al. (2012). Synthesis and characterization of new iridium photosensitizers for catalytic hydrogen generation from water. Chem. Eur. J. 18: 3220-3225.
- 77 Deisenhofer, J. and Norris, J.R. (1993). The Photosynthetic Reaction Center. San Diego, CA: Academic Press.
- **78** Blankenship, R.E. (2014). *Molecular Mechanisms of Photosynthesis*, 2e, xv. Chichester, UK: Wiley, 296 p.
- 79 Marcus, R.A. (1964). Chemical + electrochemical electron-transfer theory. Ann. Rev. Phys. Chem. 15: 155-196.
- 80 Bard, A.J. and Faulkner, L.R. (2001). Electrochemical Methods: Fundamentals and Applications, 2e, xxi, 833. New York: Wiley.
- 81 Mayer, J.M. (2004). Proton-coupled electron transfer: a reaction chemist's view. Ann. Rev. Phys. Chem. 55: 363-390.
- 82 Trasatti, S. (1972). Work function, electronegativity, and electrochemical behavior of metals 3. Electrolytic hydrogen evolution in acid solutions. J. Electroanal. Chem. 39: 163-184.
- 83 Trasatti, S. (1980). Electrocatalysis by oxides attempt at a unifying approach. J. Electroanal. Chem. 111: 125-131.
- 84 Man, I.C., Su, H.Y., Calle-Vallejo, F. et al. (2011). Universality in oxygen evolution electrocatalysis on oxide surfaces. ChemCatChem 3: 1159-1165.
- 85 Zhao, J., Holmes, M.A., and Osterloh, F.E. (2013). Quantum confinement controls photocatalysis - a free energy analysis for photocatalytic proton reduction at CdSe nanocrystals. ACS Nano 7: 4316-4325.
- 86 Zhong, D.K., Choi, S., and Gamelin, D.R. (2011). Near-complete suppression of surface recombination in solar photoelectrolysis by "Co-Pi" catalyst-modified W:BiVO₄. J. Am. Chem. Soc. 133: 18370-18377.
- 87 Osterloh, F.E. (2008). Inorganic materials as catalysts for photochemical splitting of water. Chem. Mater. 20: 35-54.
- 88 Osterloh, F.E. (2013). Inorganic nanostructures for photoelectrochemical and photocatalytic water splitting. Chem. Soc. Rev. 42: 2294-2320.
- 89 Maeda, K., Hashiguchi, H., Masuda, H. et al. (2008). Photocatalytic activity of $(Ga_{1-x}Zn_x)(N_{1-x}O_x)$ for visible-light-driven H-2 and O-2 evolution in the presence of sacrificial reagents. J. Phys. Chem. C 112: 3447-3452.

- 90 Kato, H., Sasaki, Y., Shirakura, N., and Kudo, A. (2013). Synthesis of highly active rhodium-doped SrTiO3 powders in Z-scheme systems for visible-light-driven photocatalytic overall water splitting. J. Mater. Chem. A 1: 12327-12333.
- 91 Dotan, H., Sivula, K., Gratzel, M. et al. (2011). Probing the photoelectrochemical properties of hematite (alpha-Fe₂O₃) electrodes using hydrogen peroxide as a hole scavenger. Energy and Environ. Sci. 4: 958-964.
- 92 Kim, T.W. and Choi, K.-S. (2014). Nanoporous BiVO₄ photoanodes with dual-layer oxygen evolution catalysts for solar water splitting. Science 343: 990-994.
- 93 Santato, C., Ulmann, M., and Augustynski, J. (2001). Photoelectrochemical properties of nanostructured tungsten trioxide films. J. Phys. Chem. B 105: 936-940.
- 94 Domen, K., Yoshimura, J., Sekine, T. et al. (1990). A novel series of photocatalysts with an ion-exchangeable layered structure of niobate. Catal. Lett. 4: 339-343.
- 95 Mills, A., Hazafy, D., Elouali, S., and O'Rourke, C. (2016). Periodate an alternative oxidant for testing potential water oxidation catalysts. J. Mater. Chem. A 4: 2863-2872.
- 96 Townsend, T.K., Sabio, E.M., Browning, N.D., and Osterloh, F.E. (2011). Photocatalytic water oxidation with suspended alpha-Fe₂O₃ particles – effects of nanoscaling. Energy Environ. Sci. 4: 4270-4275.
- 97 Nail, B.A., Fields, J.M., Zhao, J. et al. (2015). Nickel oxide particles catalyze photochemical hydrogen evolution from water—nanoscaling promotes P-type character and minority carrier extraction. ACS Nano 9: 5135-5142.
- 98 Gerischer, H. (1990). The impact of semiconductors on the concepts of electrochemistry. Electrochim. Acta: 35, 1677-1699.
- 99 Sathish, M., Viswanathan, B., and Viswanath, R.P. (2006). Alternate synthetic strategy for the preparation of CdS nanoparticles and its exploitation for water splitting. Int. J. Hydrogen Energy 31: 891-898.
- 100 Zheng, Y., Liu, J., Liang, J. et al. (2012). Graphitic carbon nitride materials: controllable synthesis and applications in fuel cells and photocatalysis. Energy Environ. Sci. 5: 6717-6731.
- 101 Cho, I.S., Chen, Z.B., Forman, A.J. et al. (2011). Branched TiO₂ nanorods for photoelectrochemical hydrogen production. Nano Lett. 11: 4978-4984.
- 102 Bae, S., Kim, S., Lee, S., and Choi, W. (2014). Dye decolorization test for the activity assessment of visible light photocatalysts: realities and limitations. Catal. Today 224: 21-28.
- 103 Gratzel, M. (2005). Solar energy conversion by dye-sensitized photovoltaic cells. Inorg. Chem. 44: 6841-6851.
- 104 Duret, A. and Gratzel, M. (2005). Visible light-induced water oxidation on mesoscopic alpha-Fe₂O₃ films made by ultrasonic spray pyrolysis. J. Phys. Chem. B 109: 17184-17191.

- 105 Chen, D.L., Gao, L., Yasumori, A. et al. (2008). Size- and shape-controlled conversion of tungstate-based inorganic-organic hybrid belts to WO₃ nanoplates with high specific surface areas. Small 4: 1813-1822.
- 106 Newton, K.A. and Osterloh, F.E. (2016). Size and morphology of suspended WO₃ particles control photochemical charge carrier extraction and photocatalytic water oxidation activity. Top. Catal. 59: 750-756.
- 107 Hagfeldt, A. and Gratzel, M. (1995). Light-induced redox reactions in nanocrystalline systems. Chem. Rev. 95: 49-68.
- 108 Shevchenko, D., Anderlund, M.F., Thapper, A., and Styring, S. (2011). Photochemical water oxidation with visible light using a cobalt containing catalyst. Energy Environ. Sci. 4: 1284-1287.
- 109 Goldsmith, J.I., Hudson, W.R., Lowry, M.S. et al. (2005). Discovery and high-throughput screening of heteroleptic iridium complexes for photoinduced hydrogen production. J. Am. Chem. Soc. 127: 7502-7510.
- 110 Wang, W.-G., Wang, F., Wang, H.-Y. et al. (2012). Electron transfer and hydrogen generation from a molecular dyad: platinum(ii) alkynyl complex anchored to [FeFe] hydrogenase subsite mimic. Dalton Trans. 41: 2420-2426.
- 111 Ott, S., Kritikos, M., Åkermark, B., and Sun, L. (2003). Synthesis and structure of a biomimetic model of the iron hydrogenase active site covalently linked to a ruthenium photosensitizer. Angew. Chem. Int. Ed. 42: 3285-3288.
- 112 Shockley, W. (1949). The theory of p-n junctions in semiconductors and p-n junction transistors. Bell Syst. Tech. J. 28: 435-489.
- 113 Gerischer, H. (1966). Electrochemical behavior of semiconductors under illumination. J. Electrochem. Soc. 113: 1174-1182.
- 114 Yang, S.Y., Martin, L.W., Byrnes, S.J. et al. (2009). Photovoltaic effects in BiFeO₃. Appl. Phys. Lett. 95: 062909.
- 115 Abdi, F.F., Han, L.H., Smets, A.H.M. et al. (2013). Efficient solar water splitting by enhanced charge separation in a bismuth vanadate-silicon tandem photoelectrode. Nat. Commun. 4: 2195.
- 116 Sander, M., Jaegermann, W., and Lewerenz, H.J. (1992). Site-specific surface interaction of adsorbed water and halogens on copper indium selenide (CuInSe₂) surfaces. J. Phys. Chem. C 96: 782–790.
- 117 Hingston, F.J., Atkinson, R.J., Posner, A.M., and Quirk, J.P. (1967). Specific adsorption of anions. Nature 215: 1459-1461.
- 118 Osterloh, F.E. (2014). Maximum theoretical efficiency limit of photovoltaic devices: effect of band structure on excited state entropy. J. Phys. Chem. Lett.: 3354-3359.
- 119 Huda, M.N., Al-Jassim, M.M., and Turner, J.A. (2011). Mott insulators: an early selection criterion for materials for photoelectrochemical H(2) production. J. Renew. Sustain. Energy 3: 053101-1-053101-10.
- 120 Green, M.A., Emery, K., Hishikawa, Y. et al. (2015). Solar cell efficiency tables (version 45). Prog. Photovolt. Res. Appl. 23: 1-9.
- 121 Madelung, O. (2004). Semiconductors: Data Handbook, 3e, 691. Berlin: Springer.

- 122 Boettcher, S.W., Warren, E.L., Putnam, M.C. et al. (2011). Photoelectrochemical hydrogen evolution using Si microwire arrays. J. Am. Chem. Soc. 133: 1216-1219.
- 123 Abdi, F.F., Firet, N., and van de Krol, R. (2013). Efficient BiVO₄ thin film photoanodes modified with cobalt phosphate catalyst and W-doping. Chem-CatChem 5: 490-496.
- 124 Glasscock, J.A., Barnes, P.R.F., Plumb, I.C., and Savvides, N. (2007). Enhancement of photoelectrochemical hydrogen production from hematite thin films by the introduction of Ti and Si. J. Phys. Chem. C 111: 16477-16488.
- 125 Liang, Y.Q., Enache, C.S., and van de Krol, R. (2008). Photoelectrochemical characterization of sprayed alpha-Fe₂O₃ thin films: influence of Si doping and SnO(2) interfacial layer. Int. J. Photoenergy: 739864, doi:https://doi.org/10.1155/ 2008/739864.
- 126 Townsend, T.K., Browning, N.D., and Osterloh, F.E. (2012). Nanoscale strontium titanate photocatalysts for overall water splitting. ACS Nano 6: 7420-7426.
- 127 Modestino, M.A., Walczak, K.A., Berger, A. et al. (2014). Robust production of purified H-2 in a stable, self-regulating, and continuously operating solar fuel generator. Energy Environ. Sci. 7: 297-301.
- 128 Osterloh, F.E. (2016). The low concentration of CO₂ in the atmosphere is an obstacle to a sustainable artificial photosynthesis fuel cycle based on carbon. ACS Energy Lett. 1: 1060-1061.
- 129 Maeda, K., Teramura, K., Lu, D.L. et al. (2006). Noble-metal/Cr₂O₃ core/shell nanoparticles as a cocatalyst for photocatalytic overall water splitting. Angew. Chem. Int. Ed. Engl. 45: 7806-7809.
- 130 Hisatomi, T., Maeda, K., Takanabe, K. et al. (2009). Aspects of the water splitting mechanism on $(Ga_{1-x}Zn_x)(N_{1-x}O_x)$ photocatalyst modified with $Rh_{2-\nu}Cr_{\nu}O_3$ cocatalyst. J. Phys. Chem. C 113: 21458-21466.
- 131 Takata, T. and Domen, K. (2009). Defect engineering of photocatalysts by doping of aliovalent metal cations for efficient water splitting. J. Phys. Chem. C 113: 19386-19388.
- 132 Ham, Y., Hisatomi, T., Goto, Y. et al. (2016). Flux-mediated doping of SrTiO₃ photocatalysts for efficient overall water splitting. J. Mater. Chem. A 4: 3027-3033.
- 133 Lee, Y.G., Teramura, K., Hara, M., and Domen, K. (2007). Modification of (Zn_{1+x}Ge)(N₂O_x) solid solution as a visible light driven photocatalyst for overall water splitting. Chem. Mater. 19: 2120-2127.
- 134 Takata, T., Pan, C., Nakabayashi, M. et al. (2015). Fabrication of a core-shelltype photocatalyst via photodeposition of group IV and V transition metal oxyhydroxides: an effective surface modification method for overall water splitting. J. Am. Chem. Soc. 137: 9627-9634.
- 135 Kato, H., Sasaki, Y., Wase, A., and Kudo, A. (2007). Role of iron ion electron mediator on photocatalytic overall water splitting under visible light irradiation using Z-scheme systems. Bull. Chem. Soc. Jpn. 80: 2457-2464.

- $\bf 136\,$ Arakawa, H. (2002). Water photolysis by ${\rm TiO_2}$ particles-significant effect of Na2CO3 addition on water splitting. In: Photocatalysis Science and Technology (eds. M. Kaneko and I. Okura), 235-248. New York: Springer.
- 137 Abe, R., Sayama, K., and Arakawa, H. (2003). Significant effect of iodide addition on water splitting into H₂ and O₂ over Pt-loaded TiO₂ photocatalyst: suppression of backward reaction. Chem. Phys. Lett. 371: 360-364.